Directed evolution for cell separation in natural isolates of budding yeast reveals negative selection on *AMN1* and the Rim101 pathway in haploids and positive selection for Hawthorne's deletion in diploids

Benjamin Galeota-Sprung[1a], Erik Pritchard[2], Crystal Huang[2], Amy Fernandez[2], and Paul Sniegowski[3]

[1] University of Pennsylvania Perelman School of Medicine
[2] University of Pennsylvania Department of Biology
[3] Earlham College
[a] Corresponding author

Abstract

Natural isolates of the yeast *Saccharomyces cerevisiae* were evolved under a transfer protocol that selected for cell separation and against clumpy growth. Whole-genome sequencing of haploid populations revealed strong selection to deactivate *AMN1*, a known regulator of cell separation, as well as multiple instances of loss-of-function mutations on the Rim101 pathway and the gene *STE11*. The Rim101 pathway's role as a major regulator of cell separation has likely been masked, heretofore, by the nonfunctional allele of *AMN1* carried by common laboratory strains. Haploid populations were characterized by multiple competing lineages. In diploid populations, we observed repeated large partial deletions of chromosome III involving fusions of the mating-type loci, the so-called Hawthorne's deletion. We measured the spontaneous rate of Hawthorne's deletion and found that it is within an order of magnitude of previously measured rates of whole-chromosome aneuploidy.

Introduction

Cell aggregation phenotypes in the yeast *S. cerevisiae* include flocculation, pseudohyphal growth, invasive growth, biofilms, and clumpy growth (Soares, 2011). Clumpy growth, also called chain formation (Stewart, 2009), is a phenomenon in which growing cells do not fully separate after budding, leading to clusters of related cells. (In contrast to clumpy growth, flocculation is reversible, fast-acting, and not dependent on relatedness.) Typical laboratory strains of yeast are not clumpy, with much of the variation in clumpiness across strains explained by different alleles of the cell separation regulator *AMN1* (Li *et al.*, 2013). In contrast to laboratory strains, natural isolates ("wild strains") of *S. cerevisiae* are often clumpy growers, especially as haploids (Fig. 1B). Wild strains tend to be more robust than lab strains in many respects, including faster growth rate, higher sporulation efficiency, and lower rate of petite production (Dimitrov *et al.*, 2009). A barrier to the use of wild strains in laboratory work is that clumpy growth presents technical difficulties for otherwise routine assays such as dilution plating to estimate population size and flow cytometry of single cells. Evolution experiments in which selection pressure favors an aggregation phenotype have been carried out (Ratcliff *et al.*, 2015; Hope *et al.*, 2017). Here we report the results of an evolution experiment in which we selected for increased cell separation. We evolved replicate populations of wild haploid and diploid strains for 57 days under a daily transfer protocol that selected against large clumps and for separated cells.

Methods

Medium and growth conditions

The evolution experiment was carried out in glass 50 mL Erlenmeyer-type flasks containing 10 mL synthetic defined (SD) medium (6.7 g/L yeast nitrogen base, 2% glucose) supplemented with ampicillin and tetracycline, at 30 C and shaken at 200 rpm. SD was chosen as the medium for the evolution experiment because cultures of the wild diploid strains used are already very well-separated in YPD after the exponential growth phase. For haploid clones isolated from the evolution experiment, some assays were carried out in YPD (2% peptone, 1% yeast extract, 2% glucose).

Strains

The diploid strain YPS602 is a monosporic isolate of YPS133, which was isolated from Tyler Arboretum, Pennsylvania, as described previously (Sniegowski, Dombrowski and Fingerman, 2002). The closely related diploid strain YPS606 is a monosporic isolate of YPS142, also isolated from Tyler Arboretum. Both strains are related to the more widely known YPS128, and are members of the North American Oak clade (Peter *et al.*, 2018). YPS2070 is a haploid *MATα* heterothallic *(ho::kanMX)* derivative of YPS602 and YPS2055 is a haploid *MATa* heterothallic *(ho::kanMX)* derivative of YPS606.

Evolution experiment

Four replicate populations of each of the 4 strains described above were founded from single colonies and transferred daily according to the following protocol: a 2 mL aliquot of well-mixed culture was removed to a small glass tube and allowed to settle undisturbed for 10 min (Day 1 – Day 8), 20 min (Day 9 – Day 14), or 30 min (Day 15 – Day 57). After the waiting period, 100 µL of culture was carefully removed from near the top of the aliquot and transferred to 9.9 mL fresh medium in a new flask.

Transfers were performed every ~24h for 57 days. At regular intervals, 3 mL of culture was frozen in 15% glycerol and stored at -80 C. Also at regular intervals, the number of cells transferred was estimated by hemocytometer count. Clonal isolates were obtained from frozen population samples by streaking to single colonies. For a control (no selection against clumping) evolution experiment, conditions were identical except that 50 µl of well-mixed culture was added to 9.95 mL fresh medium at each transfer, for 66 days.

Populations analyzed

The 16 populations founded from the haploids YPS2070 and YPS2055 and the diploids YPS602 and YPS606 were designated H1-H4, H5-H8, D1-D4, and D5-D8, respectively. After completion of the evolution experiment, it became apparent that at some point between days 29 and 35, the diploid populations D5-D8 were inadvertently discontinued while haploid populations H5-H8 were duplicated. We subsequently adopted an *a/b* naming scheme to distinguish these duplicated populations. Population H4 was lost before the end of the experiment due to a separate technical error. Therefore after 57 days of evolution there were 11 haploid populations (H1, H2, H3, H5a, H5b, H6a, H6b, H7a, H7b, H8a, H8b) and 4 diploid populations (D1, D2, D3, D4) available for analysis, and additionally the diploid populations D5-D8 completed 29 days of evolution.

Settling and sedimentation assays

When a well-mixed culture of yeast is placed in a clear vessel and allowed to settle, two phenomena are apparent: (1) sediment collects at the bottom of the vessel and (2) the cloudy area of culture suspension moves visibly downwards, with clear medium above. We measured both manifestations of settling (for illustrative photographs of settling see Figure S2). Haploid assays were performed in YPD while diploid

assays were performed in SD. For all assays, clones were started from a frozen chunk and grown overnight in YPD, and then grown for two 24h cycles in SD or one 24h cycle in YPD, diluting 1/100 at each transfer, prior to the assay. In the sedimentation assays, 5 mL of well-mixed culture was placed into a 15 mL conical tube suspended vertically; after two hours, the height of the sediment at the bottom was measured to the nearest tenth of a millimeter using a digital caliper tool. This height was subsequently converted to a volume. For haploids, the settling distance was measured concurrently with the sediment measurement, from the same 5 mL aliquot, estimated as the distance from the meniscus to the midpoint between clear media and cloudiest culture. For diploids, the settling distance was measured by a slightly different procedure: 900 µl of culture was briefly spun down (90 s at 10,000 rcf) and resuspended in 900 µl sterile water. Then 700 µl of this resuspension was pipetted into a narrow-profile cuvette and allowed to settle. We used cuvettes because we found that the flat surface aided in accurate measurement, and the resuspension step was necessary because cultures in SD do not settle evenly. After 2 hours, the downward progression of the visible demarcation from clear to cloudy was measured to the nearest tenth of a millimeter using a digital caliper tool.

DNA extraction and whole-genome sequencing

We used the genome assembly of YPS128 as provided by (Yue *et al.*, 2017) as the reference for all genomic analyses described here. For clones, a culture was started from a frozen chunk, while for frozen populations, the entire frozen sample was thawed and 10 µl used to inoculate a new culture. After growth overnight in YPD, DNA was extracted from 1 mL of culture using kit D7005 from Zymo Research. Short-read whole-genome sequencing was performed on an Illumina NovaSeq X Plus sequencer in one or more multiplexed shared-flow-cell runs, producing 2x151bp paired-end reads. Reads were mapped to the reference genome using `bwa mem` (Li, 2013), and duplicate reads removed by `PicardTools MarkDuplicates`. Mutations were called using `freebayes` (Garrison and Marth, 2012) on the default settings, with all potential variants reviewed manually and examined in IGV (Robinson *et al.*, 2011). Mutation calls from this pipeline were also spot-checked using `breseq` (Deatherage and Barrick, 2014). For the allele frequencies shown in Table 1, all alleles with at least two reads were considered. To locate chromosomal deletions, plots of read depth were created from the output of `samtools -depth` (Danecek *et al.*, 2021). Additionally, long-read Nanopore sequencing was used to confirm the MAT-HML fusion in the clone isolated from population D2. To do so, we used `blastn` (Camacho *et al.*, 2009) to map segments of genes bordering HML and MAT to all Nanopore reads >= 10 kb that mapped to chrIII, from which we detected single reads spanning both regions as evidence of fusion.

Allele replacements

We replaced *AMN1* alleles in evolved clones with the ancestral *AMN1* sequence. To do so we inserted the *natMX* cassette just downstream of *AMN1* in the ancestral strain. We then amplified the entire *AMN1-natMX* cassette and transformed it into evolved strains. Successful transformation was confirmed first by PCR amplicon size and then by Sanger sequencing to ensure that the ancestral allele was introduced. Transformations were carried out by standard lithium acetate methods (Gietz and Schiestl, 2007).

Cluster size analysis

While microscopic inspection of evolved haploid strains showed a clear and obvious cell separation phenotype (Fig 1B), for diploids the phenotype was more subtle. To estimate the distribution of cluster sizes in diploid strains, we employed the following procedure. A frozen chunk of the strain of interest was used to inoculate an overnight culture in YPD; the following day this culture was diluted 1/100 into fresh

124 SD and allowed to grow for 24 h; then another 1/100 dilution and growth cycle in SD was performed;
125 and finally on the 4th day 200 µl of culture was transferred to 12 mL fresh SD and grown until A600=0.6,
126 at which point photographs of the culture were taken at 100× magnification. Subsequently, the number
127 of cells in each cluster was manually labelled (example shown in Figure S4) and recorded for further
128 analysis.

129 *Sporulation and tetrad dissection*
130 Sporulation and tetrad dissection were carried out by standard methods.

131 *PCR verification of Hawthorne's deletion*
132 Primers 5'-TGGAAAGCGTAAACACGGAG-3' and 5'-TCGGATTTGCGCTTGACAAT-3' were used to verify the
133 MAT-HMR deletion; these primers produce an amplicon of ~3.5 kbp only in the case of a MAT-HMR
134 fusion. Similarly, primers 5'-GTCCAGGGGCGGTTTATTTT-3' and 5'-GGACTTGGAAGAAGCGTTGG-3' were
135 used to verify the MAT-HML deletion. Both primer sets were validated on known Hawthorne's deletion
136 strains as determined by whole-genome sequencing.

137 *Estimation of the spontaneous rate of Hawthorne's deletion*
138 In order to carry out a fluctuation assay to estimate the rate of MAT-HMR deletion, we constructed the
139 following heterothallic haploid strains in the YPS602 background. YPS4277 has the genotype *MATalpha*
140 *ho::hphMX ura3::natMX his4::kanMX THR4*. YPS4263 has the genotype *MATa ho::hphMX ura3::natMX*
141 *HIS4 thr4::URA3 amdSYM* with the *amdSYM* marker (Solis-Escalante *et al.*, 2013) inserted on chrIII
142 between *SED4* and *ATG15*. These strains were constructed by standard lithium acetate transformation
143 methods. We then mated these strains creating the diploid YPS4283, which is sensitive to both 5-
144 fluoroorotic acid (5-FOA) and fluoroacetamide (FAA). The markers responsible for the sensitivity were
145 located on chrIII between MAT and HMR, so that a MAT-HMR deletion created a double 5-FOA/FAA
146 resistant, while complete loss of the marked chrIII from this strain caused histidine auxotrophy that was
147 easily selected against by the absence of histidine in the medium.

148 We inoculated 4 replicate cultures from single colonies of YPS4283 into 6 mL SD + 20 mg/L uracil. The
149 cultures were grown overnight at 30 C with shaking, the density estimated by hemocytometer and a
150 target of 1000 cells transferred to 10 mL fresh SD + uracil. These sub-cultures were grown for 3 days at
151 30 C with shaking, at which time density was estimated by hemocytometer and 40 µL (1/250th of the
152 culture) was plated neat to SD + uracil + 1 g/L FOA + 2.3 g/L FAA agar plates. Plates were incubated for 2
153 days at 30 C and then examined. Very small colonies were excluded from subsequent analysis. From each
154 plate, 32-38 colonies were picked to both 1 mL YPD and to 1 mL SPO+uracil, in glass tubes. The YPD
155 cultures were grown overnight and then stored at 4 C until needed. The SPO + uracil cultures were
156 grown at 30 C for 3 days and then examined via microscope. From any culture in which sporulation was
157 observed, at least 4 tetrads were dissected. If the dissection yielded a consistent pattern of 2:2 live:dead,
158 DNA was extracted from the corresponding YPD culture and a MAT-HMR deletion was verified via PCR.
159 The total number of verified MAT-HMR deletions for each replicate (Table S2) was input into the package
160 rSalvador (Zheng, 2017), using the Lea-Coulson model with ε=1/250, to generate a point estimate and
161 confidence interval for the spontaneous rate of MAT-HMR deletion.

162

Results

All evolved haploid clones had a mutation to AMN1 or to the Rim101 pathway

We isolated one clone from each final haploid population. All clones isolated from haploid Day 57 populations were markedly less clumpy when examined microscopically (examples shown in Fig. 1B), and displayed changes of large and statistically significant magnitude in two assays measuring settling (Figs. 1C and 1D). Whole-genome sequencing revealed that all clones had either a mutation to *AMN1*, a known regulator of cell separation, or a gene in the Rim101 pathway: *RIM8, RIM13, RIM20,* or *RIM101*. There were no *AMN1* / Rim101 pathway double mutants.

All AMN1 and Rim101 pathway mutations appeared to be loss-of-function

In total we observed 10 independent *AMN1* mutations (Fig. 1E and Table 1). Of these, 7 are nonsense or frameshift while 3 are amino acid substitutions. Of note, the 3 substitutions all occur in between residues 452-472. Similarly, of the 4 mutations observed in the Rim101 pathway, three are frameshift or nonsense mutations and one is a substitution. Our supposition was that all *AMN1* and Rim101 pathway mutations, including the substitutions, were loss of function. We investigated two AMN1 substitutions more closely: in the respective evolved clones, we replaced $AMN1^{C452Y}$ and $AMN1^{L472P}$ with the ancestral allele. These replacements completely restored the clumpy phenotype (Fig. S1), demonstrating that the substitutions alone were sufficient to cause the separated phenotype.

The phenotype of AMN1 and Rim101 pathway mutations differs

While the gross appearance of *AMN1* and Rim101 pathway mutants and knockouts is similar in that both appear far less clumpy than the ancestor (e.g. Fig. 1B), the settling assays reveal differences. We allowed cultures to rest undisturbed for 2 h and measured two different aspects of the process of cells settling out of solution (see Methods). Comparing group means, *AMN1* mutants accumulate more sediment at the bottom of the culture than do Rim101 pathway mutants (168.3 mm^3 vs 114.9 mm^3, $p < 1e\text{-}04$; Fig. 1C). Conversely, in Rim101 pathway mutants, more downwards progress of the visibly cloudy area of culture (5.6 mm vs 4.7 mm, $p < 1e\text{-}06$; Fig. 1D) is observed than in *AMN1* mutants.

Haploid populations were diverse and experienced soft sweeps

Pairs of clones isolated from populations that were originally a single population tended to have different *AMN1* or Rim101 pathway mutations (Fig. 1E noting *a* and *b* labels). This suggested that populations were diverse, with many contending lineages. To confirm this, we performed whole-population sequencing of haploid populations H3 and H5a. The results (Table 1) confirmed our hypothesis: we detected at least 6 independent *AMN1* or Rim101p mutant lineages across the two populations. We also suspect there are further low-frequency lineages that we were unable to resolve due to limitations of read depth.

Parallel loss-of-function mutations to STE11 occurred in haploids

In the sequenced haploid clones we observed three independent mutations to *STE11*, each of which all appeared in conjunction with an *AMN1* or Rim101p pathway mutation. We confirmed that these clones are sterile (do not mate), as expected for loss-of-function mutations. Because populations H7a and H7b were once a single population and share the mutation $AMN1^{D373*}$, we can infer with relative confidence that the $STE11^{C430*}$ mutation arose in a background that already had fixed $AMN1^{D373*}$. We surmise, then, that all observed *STE11* mutations were second mutations. Settling and sedimentation assays did not detect an effect of knocking out *STE11*; however, we did notice a subtle visual difference in settling

204 appearance. It remains uncertain whether *ste11* mutations rose in frequency in response to the selection
205 for cell separation, or whether they had a more general effect on fitness in the experiment.

206 *Large deletions involving the mating loci evolved multiple times in diploid populations*
207 In contrast to haploid populations, in which all mutations affecting the cell separation phenotype that we
208 detected were single-base-pair point mutations, in diploid populations we found that a large deletion on
209 chromosome III evolved repeatedly (Fig. 2A). This ~90 kb deletion (about 30% of chrIII) spans the region
210 from MAT to HMR, or, in one case, the region from MAT to HML (~125 kb, or about 40% of chrIII). Clones
211 with this deletion segregated 2 live:2 dead spores upon dissection of tetrads, consistent with the
212 presence of multiple essential genes present on the deleted segment. This deletion is historically known
213 as Hawthorne's deletion (Herskowitz, 1988). Clones with the MAT-HMR or MAT-HML deletion exhibited
214 significantly less sedimentation than the ancestor (Fig. 2C), and an analysis of the distribution of cluster
215 size showed that they were less clumpy than the ancestor (Fig. 3A). For example, the ancestral
216 proportion of cells occurring in clumps of 4 cells or fewer was 43%; for the Hawthorne's deletion strains,
217 this estimate ranged from 65% to 77%. Whole-population sequencing of populations D1, D2, and D4 at
218 Day 57 revealed that this macromutation, or segmental aneuploidy, was fixed or nearly fixed. We also
219 found evidence for the presence of this deletion in 3 of 4 Day 29 populations (D5, D6, and D8; Fig. S5), so
220 that in total a Hawthorne's deletion was observed in 6 of 8 diploid populations.

221 *Curing the deletion restores the ancestral phenotype*
222 The live products of dissected tetrads from the Hawthorne's deletion strains, being homothallic, yielded
223 diploid colonies cured of the deletion. These derived diploids no longer showed the reduced-
224 sedimentation phenotype displayed in the strains with the deletion (Fig. 2D).

225 *Hawthorne's deletions were not observed in a control experiment*
226 We wished to rule out that the Hawthorne's deletion was unconditionally beneficial in the experimental
227 environment. Therefore we carried out a control evolution experiment under the same conditions as the
228 main experiment, except that there was no selection against settling. In these populations, we observed
229 no sign of Hawthorne's deletion (Fig. S5).

230 *No adverse effect of a MAT-HML fusion was observed*
231 A MAT-HML fusion would be expected to produce a ring chromosome III (Fig. 2B) which should depress
232 spore viability below 50% because crossovers during meiosis between the ring and the linear homolog
233 are expected to generate aberrant products. The following evidence points to the existence of a ring
234 chromosome III: (1) a PCR product spanning MAT and HML is produced; (2) we performed long-read
235 sequencing and found approximately the expected number of long reads mapped to regions left of MAT
236 and right of HML (Fig. S4); and (3) neither short- nor long-read sequencing suggested a new breakage
237 site. Yet surprisingly we did not observe any reduction in spore viability below 50% (Table S1). Further
238 exploration will be necessary to determine why the expected depression in spore viability is not
239 observed.

240 *Rate of Hawthorne's deletion*
241 The time to fixation of a mutation under positive selection depends on both the strength of selection
242 and the rate of mutation. For rare mutations, there may be a substantial waiting time and even when the
243 mutation occurs, selection does not act deterministically until the lineage is of a certain size. An interest
244 in such evolutionary dynamics led us to measure the spontaneous rate of Hawthorne's deletion. To do so
245 we employed the classic fluctuation assay, using genetic modifications (described in Methods and Fig.

3C) to facilitate selection for MAT-HMR deletions while counter-selecting again the complete loss of chrIII. We found a spontaneous rate of loss of MAT-HMR of 2.9e-07 (95% CI: 4.1e-08 to 3.4e-07). This rate represents the generation of MAT-HMR fusions from a single marked copy of chrIII, so the total rate of MAT-HMR fusions is twice as large, and the total rate of any Hawthorne's deletion including MAT-HML fusions is, by implication, up to four times the measured rate, although we did not measure the rate of MAT-HML fusion.

Hawthorne's deletion mutants have an altered budding pattern

The mechanism by which Hawthorne's deletion causes increased cell separation is not clear but we suspect that it may be related to budding pattern. Diploid yeast tend to bud from alternating poles (Chant and Pringle, 1995). There are two genes between *MAT* and *HMR* that influence the budding pattern: *BUD23* and *BUD31*. Homozygous null mutants for either of these display random budding patterns (Ni and Snyder, 2001). We observed growing cells microscopically and scored whether two consecutive buddings occurred on alternate poles, and found a significant depression in the frequency of alternate-pole budding for the Hawthorne's deletion strains (Table S3), suggesting haploinsufficiency of one or both of *BUD23* and *BUD31* and a possible mechanism of action.

A dominant point mutation also produces less clumpy growth in diploids

Diploid population D3 did not have a high-frequency Hawthorne's deletion. The representative clone that we isolated had only one called mutation, a nonsynonymous heterozygous mutation (F994L) to the voltage-gated calcium channel gene *CCH1*. Population sequencing revealed this mutation fixed or at high frequency (Fig. S6). The representative isolated clone sedimented significantly less than the ancestor (Fig. 2C) and was quantitatively less clumpy (Fig. 3A). We sporulated and dissected tetrads of this isolate to produce F994L/F994L and F994F/F994F homozygotes, the genotypes of which were confirmed by Sanger sequencing. The F994F/F994F homozygotes did not show a reduced sedimentation phenotype, while the F994L/F994L homozygotes displayed a sedimentation phenotype very similar to the Hawthorne's deletion strains (Fig. 3E). The sedimentation phenotype of the F994L/F994L homozygote is not more extreme than that of the F994L/F994F heterozygote, implying that this mutation is dominant. We noticed when carrying out dissections that F994L colonies were smaller than F994F colonies, suggesting that under this experiment's particular selection regime, the heterozygote has the highest total fitness considering both growth rate and selection for cell separation.

Discussion

Selection on AMN1 in haploids was predictable

Some outcomes observed in this evolution experiment were relatively predictable. How *AMN1* regulates clumpy growth in haploids was dissected in detail by (Fang *et al.*, 2018). It is likely that semi-inadvertent selection for *AMN1* mutants is part of the evolutionary history of common lab strains, since cultures of well-separated cells are more experimentally tractable for various purposes. This experiment has in effect recapitulated that selection; thus it is not surprising that we recovered many *AMN1* mutants, although we did not observe the particular *AMN1* allele, 368V, that is present in S288C and related strains. It is a demonstration of the usefulness of experimental evolution in genotype-to-phenotype mapping—given that a selection gradient relevant to the phenotype of interest can be applied—that had *AMN1*'s role in governing cell separation in haploids *not* been known this experiment would have clearly pointed towards it.

The finding that the Rim101 pathway regulates cell separation in vegetative growth is novel

The multiple hits to the Rim101 pathway are less expected. This pathway is known to have a role in pH sensing (Yan *et al.*, 2020) and regulation of cell size (Shimasawa *et al.*, 2023), and to connect to pathways regulating filamentous growth (Cullen and Sprague, 2012). (Arras *et al.*, 2022) found that Rim101 pathway genes are required for sexual aggregation, but a role in regulation of cell separation during normal physiological growth conditions has not previously been shown. We suspect that the dramatic effect of Rim101 pathway genes on cell separation has been unnoticed to date because laboratory strains are already loss of function for *AMN1*, which masks any effect on clumpy growth of disabling a Rim101 pathway gene. This illustrates the sometimes important effect of genetic background.

The Rim101 pathway also influences cell size, and knockouts are smaller in the S288C background (Shimasawa *et al.*, 2023). We did not measure cell size, but we did observe a slight but significant difference between *AMN1* mutants and Rim101 pathway mutants in settling distance (Fig. 1D), suggesting that the settling rate of individual cells differed—consistent with the notion that Rim101 pathway mutants are smaller (assuming that smaller cells settle more slowly). There is a larger difference between *AMN1* and Rim101 pathway mutants, in the opposite direction, in sedimentation (Fig. 1C), implying that Rim101 pathway mutants remain somewhat clumpier than *AMN1* mutants. Interestingly, whole-population sequencing revealed (Table 1) that at least some populations have competing *AMN1* and Rim101 pathway lineages even after 57 days of evolution. It is possible that certain uncontrolled aspects of our experimental design—e.g. how deep the pipet tip was inserted after the waiting period—influenced whether *AMN1* or Rim101 pathway mutants predominated in any particular haploid population. Strain and mating type differences could also have played a role, although we do not have the statistical power to assign any such effects.

Ploidy and gain-of-function vs loss-of-function

One motivation for this experiment was to test for differences in the genetic architecture of adaptation between diploids and haploids. It is important to note that *AMN1* is naturally inactive in a/α diploids (Fang *et al.*, 2018), and that diploids are therefore much less clumpy to start, so that ploidy is not the only important distinction between haploids and diploids in this system. Nevertheless, we hypothesized that because of considerations of ploidy, loss-of-function mutations would be relatively more frequent in haploids while gain-of-function mutations would be relatively more frequent in diploids. This appears to be true to at least some extent. All causative mutations that we found in haploids appear to be loss-of-function, disabling the function of *AMN1*, the Rim101 pathway, and *STE11*. In diploids we found only one point mutation, *CCH1 F994L*, associated with cell separation in diploids. This mutation is dominant with respect to the sedimentation phenotype, which is consistent with gain of function, but more work would be required to establish this as fact.

Hawthorne's deletion, the rate thereof, and the role of aneuploidy in adaptation

The most surprising outcome was repeated selection for MAT-HMR or MAT-HML deletions on chromosome III. These large deletions (roughly 30-40% of chrIII) arise as a consequence of homology shared by the three mating type loci. They are historically known as Hawthorne's deletion and were instrumental in the working out of the mating type switching system (Hawthorne, 1963; Haber, Rogers and McCusker, 1980; Herskowitz, 1988; Haber, 1998). Hawthorne's deletions were initially observed in the context of aberrant mating-type switching events in heterothallic (*ho*) strains. In this respect, it is interesting that we have observed these deletions in homothallic (*HO*) wild-type diploids under vegetative growth, that is, separately from any obvious context of mating type *switching* per se. Our

point estimate of the rate of MAT-HMR fusion from one copy of chrIII (3.5e-07 per generation) implies a total rate of any Hawthorne's deletion on the order of 1e-06 per generation, which for comparison is one to two orders of magnitude higher than the mutation rate to loss of function for a typical gene (Lang and Murray, 2008). As these large deletions may be considered segmental aneuploidies (or segmental monosomies), it is also illustrative to compare to rates of whole-chromosome aneuploidy. In that context, the measured rate is less than the average per-chromosome rate of aneuploidy observed in Zhu *et al.* (2014) and Sharp *et al.* (2018) (~1e-04/16 = ~6e-06), but higher than the average per-chromosome rate of reduction in copy number observed in those studies, the large majority of observed aneuploidies (~90%) being gain in copy number in both studies.

We note that our estimation of the Hawthorne's deletion rate was performed in *ho* diploids, by necessity of the process of strain construction; although *HO* is silenced in MATa/MATα diploids it is possible that leaky expression could drive a higher rate. In nature, Hawthorne's deletion is presumably selected against; and therefore the rate of such deletions may be considered to be a kind of load imposed by the three-cassette mating-type system. The long-term benefits of the mating-type system must necessarily outweigh this and other loads associated with sexual reproduction.

Aneuploidy as adaptive mechanism

Several previous evolution experiments have observed aneuploidy in *S. cerevisiae* and other yeasts in response to various selective pressures (Gresham *et al.*, 2008; Rancati *et al.*, 2008; Selmecki *et al.*, 2009; Chen *et al.*, 2012; Gilchrist and Stelkens, 2019). Most often, an increase in chromosomal copy number is observed, but there are some reports of selection for monosomy (Yang *et al.*, 2013; Barney *et al.*, 2021). It is hypothesized that adaptation via aneuploidy might be important in natural populations by providing a transient adaptive state, especially as natural isolates of S. cerevisiae tolerate aneuploidy more easily than lab strains (Muenzner *et al.*, 2024). It would be interesting to extend the evolution reported here to observe how and if this segmental aneuploidy is resolved into, or replaced by, some euploid adaptive genotype, or whether it persists.

Mechanism of action of Hawthorne's deletion

The mechanism by which Hawthorne's deletion leads to increased cell separation is not clear, but we suspect that it may act through the joint haploinsufficiency of *BUD23* and *BUD31*. Null mutants of both of these genes display random budding patterns, and we found that the Hawthorne's deletion strains, which have only one copy of each, have a more disordered budding pattern than the wild-type ancestor (Table S3). However, it is possible that the change in budding pattern is an unrelated effect of the deletion and further work will be required to connect this genotype to a phenotype affecting settling and/or cell separation.

Figures and Tables

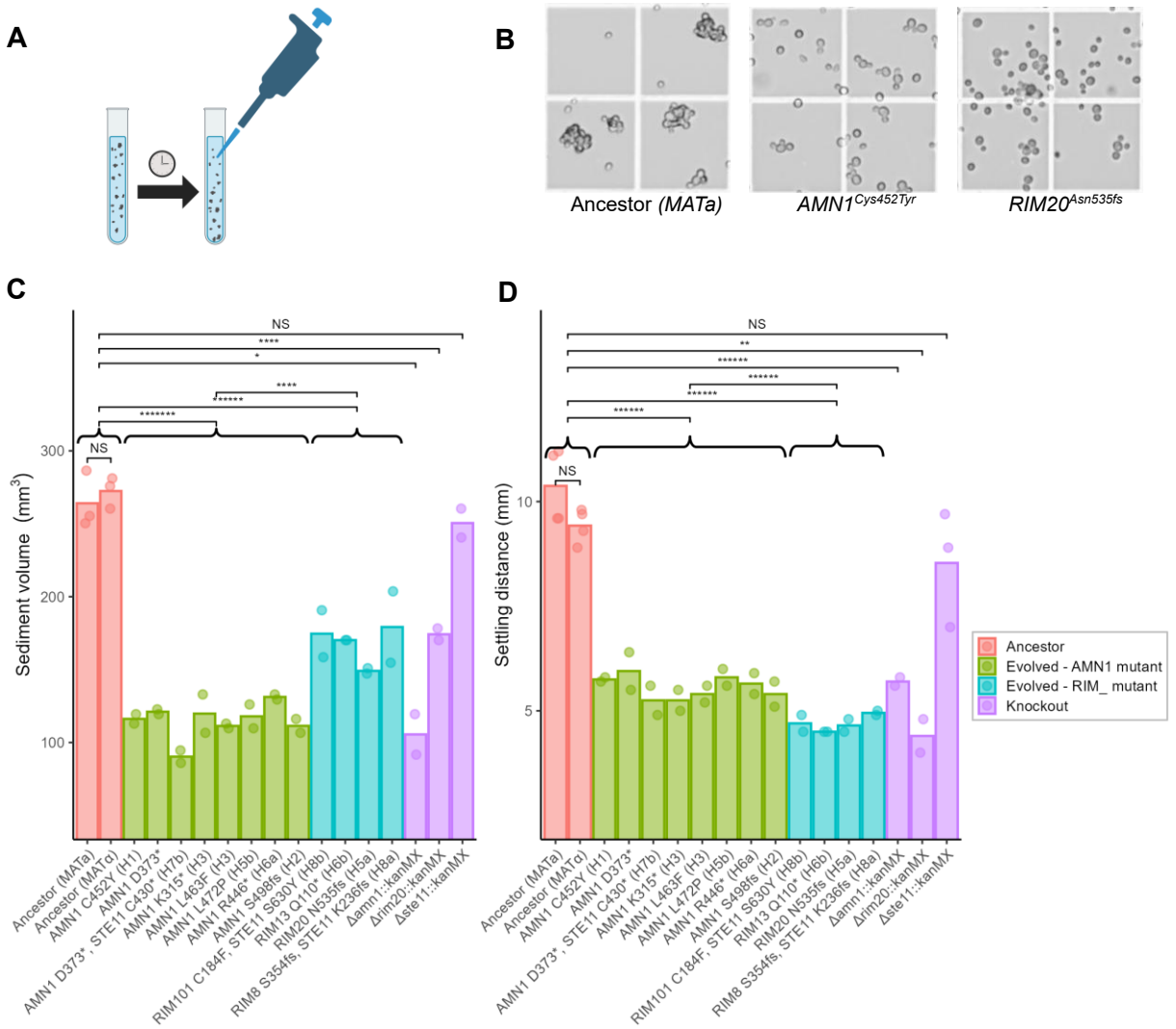

E

Gene	H1	H2	H3	H5a	H5b	H6a	H6b	H7a	H7b	H8a	H8b
AMN1	C452Y	S498fs	L463F		L472P	R446*		D373*	D373*		
RIM8										S354fs	
RIM13							Q110*				
RIM20				N535fs							
RIM101											C184F
STE11									C430*	K236fs	S630Y

Figure 1. (A) The transfer protocol allowed large clusters tend to settle out. (B) Evolved clones are far less clumpy than the ancestor. (C) Evolved and knockout haploid strains have less sediment at the bottom of a culture after 2 h of settling. (D) Evolved and knockout haploid strains have less downwards progress of the cloudy area of culture after 2h settling. Curly braces indicate group comparisons. (E) Across 11 haploid populations, parallel changes at the gene (*AMN1*, *STE11*) or pathway (Rim101) level were observed.

Haploid population H3		Haploid population H5a	
Mutation	**Freq**	**Mutation**	**Freq**
AMN1 K315*	0.51	RIM20 N535fs	0.42
AMN1 R162*	0.13	AMN1 Q224*	0.34
AMN1 E476*	0.08		
AMN1 L463F	0.07		

Table 1. Allele frequencies as revealed by whole-population sequencing of two Day 57 haploid populations.

368

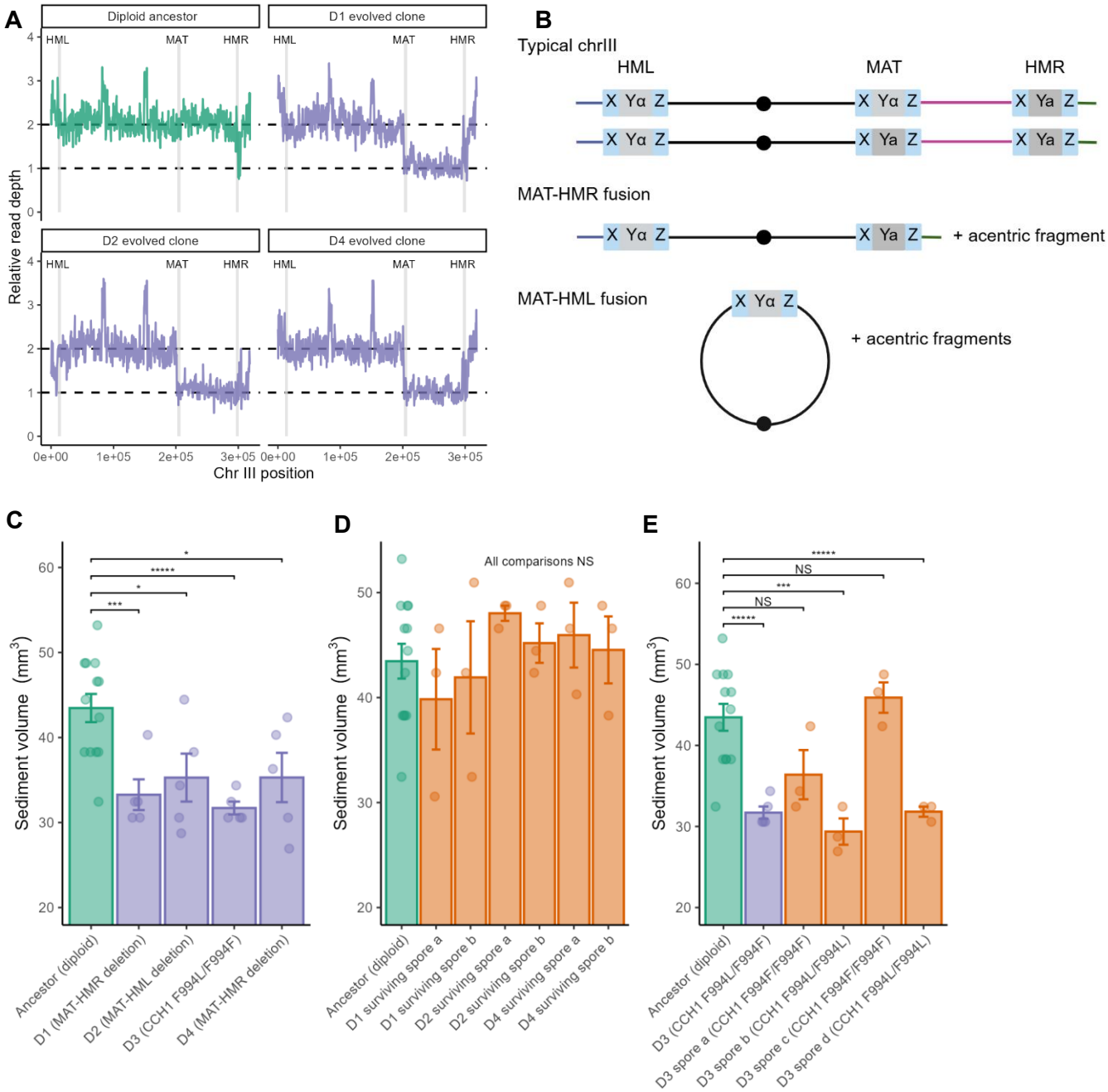

Figure 2. (A) Read depth in chromosome III showing MAT-HMR and MAT-HML deletions in clones isolated from diploid populations. (B) Schematic of the products of MAT-HMR and MAT-HML fusions. (C) Clone isolated from diploid populations have reduced sedimentation compared to the ancestor. (D) Dissection products of evolved diploid clones "cured" of their deletion have the ancestral sedimentation phenotype. (E) Dissection products of the *CCH1* heterozygote: the reduced-sedimentation phenotype segregates with the F994L homozygote.

369

370

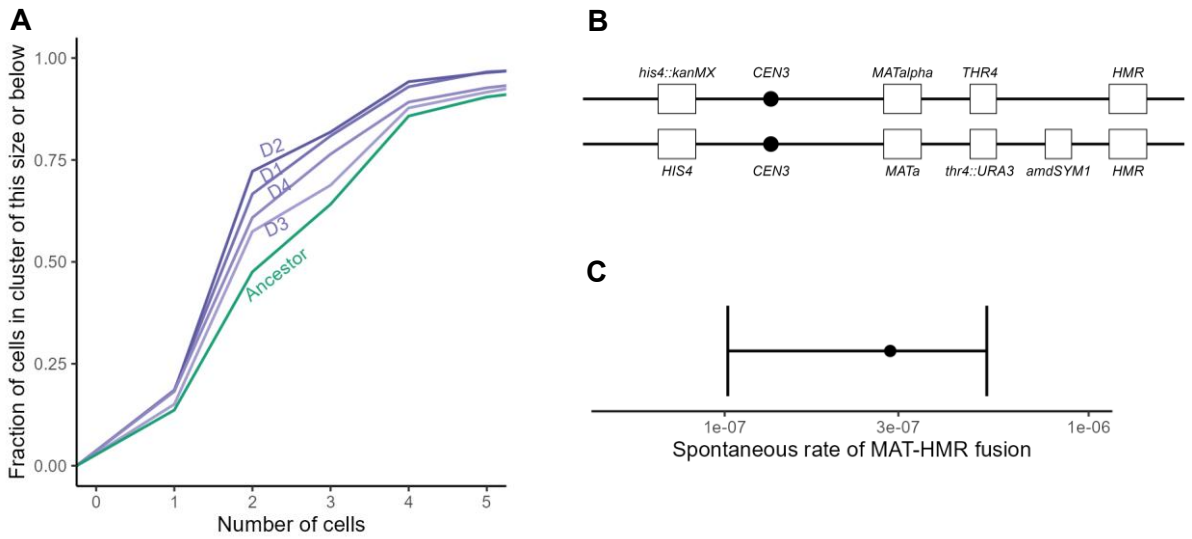

Figure 3. (A) The empirical cumulative distribution of cell cluster size for evolved diploid genotypes. (B) Selection scheme to enable estimation of the rate of Hawthorne's deletion: one copy of chrIII was doubly tagged with counterselectable markers located between *MAT* and *HMR.* Complete loss of the tagged chrIII was selected against by histidine auxotrophy. (C) The spontaneous rate of MAT-HMR deletion of one copy of chrIII as estimated by the fluctuation assay.

371

372

373

374 **References**

375 Arras, S.D.M. *et al.* (2022) “Creeping yeast: a simple, cheap and robust protocol for the identification of
376 mating type in Saccharomyces cerevisiae,” *FEMS Yeast Research*, 22(1), p. foac017. Available at:
377 https://doi.org/10.1093/femsyr/foac017.

378 Barney, J.B. *et al.* (2021) “Drug resistance in diploid yeast is acquired through dominant
379 alleles, haploinsufficiency, gene duplication and aneuploidy,” *PLoS Genetics*, 17(9), p. e1009800.
380 Available at: https://doi.org/10.1371/journal.pgen.1009800.

381 Camacho, C. *et al.* (2009) “BLAST+: architecture and applications,” *BMC bioinformatics*, 10, p. 421.
382 Available at: https://doi.org/10.1186/1471-2105-10-421.

383 Chant, J. and Pringle, J.R. (1995) “Patterns of bud-site selection in the yeast Saccharomyces cerevisiae.,”
384 *Journal of Cell Biology*, 129(3), pp. 751–765. Available at: https://doi.org/10.1083/jcb.129.3.751.

385 Chen, G. *et al.* (2012) “Hsp90 stress potentiates rapid cellular adaptation through induction of
386 aneuploidy,” *Nature*, 482(7384), pp. 246–250. Available at: https://doi.org/10.1038/nature10795.

387 Cullen, P.J. and Sprague, G.F. (2012) “The Regulation of Filamentous Growth in Yeast,” *Genetics*, 190(1),
388 pp. 23–49. Available at: https://doi.org/10.1534/genetics.111.127456.

389 Danecek, P. *et al.* (2021) “Twelve years of SAMtools and BCFtools,” *GigaScience*, 10(2), p. giab008.
390 Available at: https://doi.org/10.1093/gigascience/giab008.

391 Deatherage, D.E. and Barrick, J.E. (2014) “Identification of mutations in laboratory evolved microbes
392 from next-generation sequencing data using breseq,” *Methods in molecular biology (Clifton, N.J.)*, 1151,
393 pp. 165–188. Available at: https://doi.org/10.1007/978-1-4939-0554-6_12.

394 Fang, O. *et al.* (2018) “Amn1 governs post-mitotic cell separation in Saccharomyces cerevisiae,” *PLOS*
395 *Genetics*, 14(10), p. e1007691. Available at: https://doi.org/10.1371/journal.pgen.1007691.

396 Garrison, E. and Marth, G. (2012) “Haplotype-based variant detection from short-read sequencing.”
397 arXiv. Available at: https://doi.org/10.48550/arXiv.1207.3907.

398 Gietz, R.D. and Schiestl, R.H. (2007) “High-efficiency yeast transformation using the LiAc/SS carrier
399 DNA/PEG method,” *Nature Protocols*, 2(1), p. 31. Available at: https://doi.org/10.1038/nprot.2007.13.

400 Gilchrist, C. and Stelkens, R. (2019) “Aneuploidy in yeast: Segregation error or adaptation mechanism?,”
401 *Yeast (Chichester, England)*, 36(9), pp. 525–539. Available at: https://doi.org/10.1002/yea.3427.

402 Gresham, D. *et al.* (2008) “The Repertoire and Dynamics of Evolutionary Adaptations to Controlled
403 Nutrient-Limited Environments in Yeast,” *PLOS Genetics*, 4(12), p. e1000303. Available at:
404 https://doi.org/10.1371/journal.pgen.1000303.

405 Haber, J.E. (1998) “Mating-Type Gene Switching in Saccharomyces Cerevisiae,” *Annual Review of*
406 *Genetics*, 32(1), pp. 561–599. Available at: https://doi.org/10.1146/annurev.genet.32.1.561.

Haber, J.E., Rogers, D.T. and McCusker, J.H. (1980) “Homothallic conversions of yeast mating-type genes occur by intrachromosomal recombination,” *Cell*, 22(1, Part 1), pp. 277–289. Available at: https://doi.org/10.1016/0092-8674(80)90175-0.

Hawthorne, D.C. (1963) “A Deletion in Yeast and Its Bearing on the Structure of the Mating Type Locus,” *Genetics*, 48(12), pp. 1727–1729.

Herskowitz, I. (1988) “The Hawthorne Deletion Twenty-Five Years Later,” *Genetics*, 120(4), pp. 857–861.

Hope, E.A. *et al.* (2017) “Experimental Evolution Reveals Favored Adaptive Routes to Cell Aggregation in Yeast,” *Genetics*, 206(2), pp. 1153–1167. Available at: https://doi.org/10.1534/genetics.116.198895.

Lang, G.I. and Murray, A.W. (2008) “Estimating the per-base-pair mutation rate in the yeast Saccharomyces cerevisiae,” *Genetics*, 178(1), pp. 67–82. Available at: https://doi.org/10.1534/genetics.107.071506.

Li, H. (2013) “Aligning sequence reads, clone sequences and assembly contigs with BWA-MEM.” arXiv. Available at: https://doi.org/10.48550/arXiv.1303.3997.

Li, J. *et al.* (2013) “Polygenic Molecular Architecture Underlying Non-Sexual Cell Aggregation in Budding Yeast,” *DNA Research*, 20(1), pp. 55–66. Available at: https://doi.org/10.1093/dnares/dss033.

Muenzner, J. *et al.* (2024) “Natural proteome diversity links aneuploidy tolerance to protein turnover,” *Nature*, pp. 1–9. Available at: https://doi.org/10.1038/s41586-024-07442-9.

Ni, L. and Snyder, M. (2001) “A genomic study of the bipolar bud site selection pattern in Saccharomyces cerevisiae,” *Molecular Biology of the Cell*, 12(7), pp. 2147–2170. Available at: https://doi.org/10.1091/mbc.12.7.2147.

Peter, J. *et al.* (2018) “Genome evolution across 1,011 Saccharomyces cerevisiae isolates,” *Nature*, 556(7701), p. 339. Available at: https://doi.org/10.1038/s41586-018-0030-5.

Rancati, G. *et al.* (2008) “Aneuploidy and polyploidy underlie adaptive evolution of yeast cells deprived of a conserved cytokinesis motor,” *Cell*, 135(5), pp. 879–893. Available at: https://doi.org/10.1016/j.cell.2008.09.039.

Ratcliff, W.C. *et al.* (2015) “Origins of multicellular evolvability in snowflake yeast,” *Nature Communications*, 6(1), p. 6102. Available at: https://doi.org/10.1038/ncomms7102.

Robinson, J.T. *et al.* (2011) “Integrative Genomics Viewer,” *Nature biotechnology*, 29(1), pp. 24–26. Available at: https://doi.org/10.1038/nbt.1754.

Selmecki, A.M. *et al.* (2009) “Acquisition of Aneuploidy Provides Increased Fitness during the Evolution of Antifungal Drug Resistance,” *PLOS Genetics*, 5(10), p. e1000705. Available at: https://doi.org/10.1371/journal.pgen.1000705.

Sharp, N.P. *et al.* (2018) “The genome-wide rate and spectrum of spontaneous mutations differ between haploid and diploid yeast,” *Proceedings of the National Academy of Sciences*, 115(22), pp. E5046–E5055. Available at: https://doi.org/10.1073/pnas.1801040115.

Shimasawa, M. *et al.* (2023) “The pH-sensing Rim101 pathway regulates cell size in budding yeast,” *Journal of Biological Chemistry*, 299(3). Available at: https://doi.org/10.1016/j.jbc.2023.102973.

Sniegowski, P.D., Dombrowski, P.G. and Fingerman, E. (2002) “Saccharomyces cerevisiae and Saccharomyces paradoxus coexist in a natural woodland site in North America and display different levels of reproductive isolation from European conspecifics,” *FEMS Yeast Research*, 1(4), pp. 299–306. Available at: https://doi.org/10.1111/j.1567-1364.2002.tb00048.x.

Soares, E.V. (2011) “Flocculation in Saccharomyces cerevisiae: a review,” *Journal of Applied Microbiology*, 110(1), pp. 1–18. Available at: https://doi.org/10.1111/j.1365-2672.2010.04897.x.

Solis-Escalante, D. *et al.* (2013) “amdSYM, a new dominant recyclable marker cassette for Saccharomyces cerevisiae,” *Fems Yeast Research*, 13(1), p. 126. Available at: https://doi.org/10.1111/1567-1364.12024.

Stewart, G.G. (2009) “The Horace Brown Medal Lecture: Forty Years of Brewing Research,” *Journal of the Institute of Brewing*, 115(1), pp. 3–29. Available at: https://doi.org/10.1002/j.2050-0416.2009.tb00340.x.

Yan, H. *et al.* (2020) “The pH-sensing Rim101 pathway positively regulates the transcriptional expression of the calcium pump gene PMR1 to affect calcium sensitivity in budding yeast,” *Biochemical and Biophysical Research Communications*, 532(3), pp. 453–458. Available at: https://doi.org/10.1016/j.bbrc.2020.08.083.

Yang, F. *et al.* (2013) “Chromosome 5 Monosomy of Candida albicans Controls Susceptibility to Various Toxic Agents, Including Major Antifungals,” *Antimicrobial Agents and Chemotherapy*, 57(10), pp. 5026–5036. Available at: https://doi.org/10.1128/AAC.00516-13.

Yue, J.-X. *et al.* (2017) “Contrasting evolutionary genome dynamics between domesticated and wild yeasts,” *Nature Genetics*, 49(6), pp. 913–924. Available at: https://doi.org/10.1038/ng.3847.

Zheng, Q. (2017) “rSalvador: An R Package for the Fluctuation Experiment,” *G3: Genes|Genomes|Genetics*, 7(12), pp. 3849–3856. Available at: https://doi.org/10.1534/g3.117.300120.

Zhu, Y.O. *et al.* (2014) “Precise estimates of mutation rate and spectrum in yeast,” *Proceedings of the National Academy of Sciences*, 111(22), pp. E2310–E2318. Available at: https://doi.org/10.1073/pnas.1323011111.